Conference Volume: 22nd Conference On Radar Meteorology, 10-13 Sept. 1984, Zurich, Switzerland. Published By The Amer. Meteorological Society, Boston, Mass. USA

AIRBORNE DOPPLER RADAR OBSERVATIONS IN HURRICANE ALICIA

Frank D. Marks, Jr.
Hurricane Research Division, AOML/NOAA
Miami, Florida 33149

Robert A. Houze, Jr.
Department of Atmospheric Science
University of Washington
Seattle, Washington 98195

1. INTRODUCTION

In a study of the structure of the developing eyewall of Hurricane Debby (1982), Marks and Houze (1984) demonstrated the potential of the NOAA airborne Doppler radar for making horizontal wind measurements in tropical cyclones. That study illustrated the capability of the airborne Doppler radar to provide accurate detailed spatial coverage of the wind field in hurricanes. The Doppler wind analysis described two types of mesoscale disturbances in the developing inner-core that had not been documented before: (1) a mesocyclone, separate from the storm circulation center, located along the inside edge of the developing eyewall; and (2) two distinct windspeed maxima embedded within the developing eyewall. Both types of features were associated with mesoscale concentrations of vorticity and divergence.

During the 1983 hurricane season, airborne Doppler radar data were collected in Hurricane Alicia, which formed in the central Gulf of Mexico on 16 August 1983 [see Case and Gerrish (1983) for details of Alicia's track and development]. Airborne Doppler measurements were collected during two periods during the storm's life: one early in the Alicia's development, 15-20 h before landfall; and a second, 2-5 h before landfall. The second collection period provided an excellent opportunity to collect airborne Doppler radar data in the eyewall of a mature storm, in contrast to our study of Debby, in which the inner-core was observed by Doppler radar in its developing stages.

In this paper we concentrate on the radial and vertical structure of the eyewall of Alicia. The distributions of reflectivity, as well as, Doppler-derived tangential, radial and vertical wind components have been constructed. These results are compared with recent observational and numerical studies.

2. LARGE-SCALE STORM STRUCTURE

During the period of our analysis (0108 and 0155 GMT, 18 August 1983), Hurricane Alicia was located near 28.5°N, 94.8°W (appoximately 90 km south of Galveston, Texas), and was drifting slowly (<2 m s^{-1}) toward the west-northwest. Maximum winds at flight level (1500 m) were 50-53 m s^{-1} and the minimum central pressure was 967 mb.

Figure 1 shows the aircraft flight track (relative to the storm center) and the radar structure as viewed from the National Weather Service WSR-57 radar at Galveston. The flight track was obtained by plotting the aircraft position in a rectangular Cartesian grid with X positive to the east, Y positive to the north, and the origin (0,0) located at the storm center. The storm track was determined objectively from the aircraft flight level winds using a technique described by Willoughby and Chelmow (1982). The radar data represent instantaneous estimates of reflectivity from a single sweep (0-360 deg azimuth) mapped to the rectangular Cartesian grid centered on the storm.

Figure 1 shows that a well developed eyewall was present during the time period under consideration. The strongest reflectivity in the eyewall was 40-45 dB(Z) along the northern semicircle at a radius of 12-15 km from the storm center. This region of strong reflectivity remained relatively fixed north of the storm center throughout the 47 min period of the analysis.

3. METHODS OF ANALYSIS

As the tail radar scanned from 0 to 360 deg, vertical incidence reflectivity and Doppler radial velocity data were collected. Time-height cross sections of reflectivity and vertical velocity were constructed using the vertical incidence measurements along the flight track. Reflectivity cross sections were constructed by mapping the instantaneous reflectivity

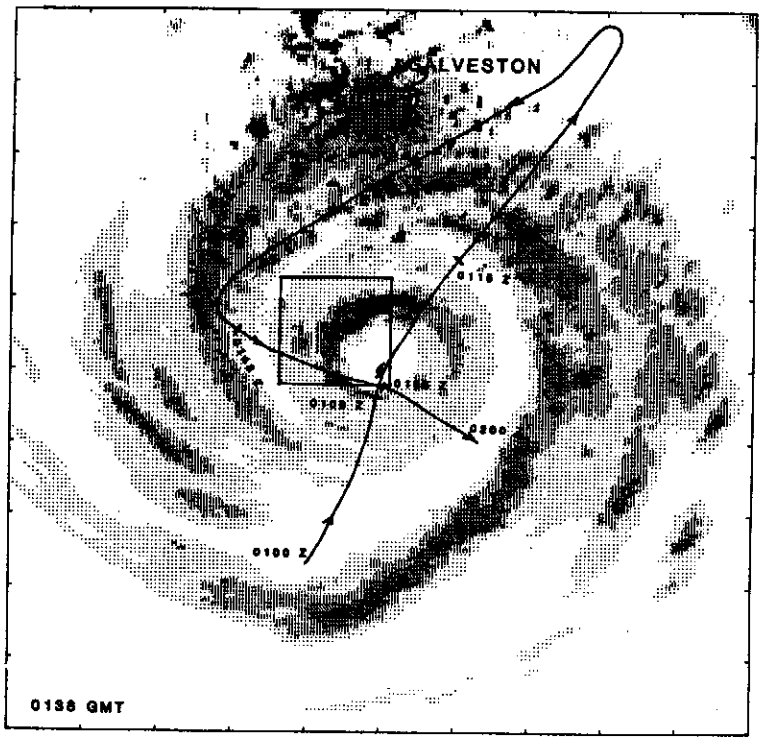

Fig. 1. Horizontal distribution of reflectivity in Hurricane Alicia from the National Weather Service WSR-57 radar at Galveston, Texas at 0138 GMT, 18 August 1983. Reflectivity contours are at 20, 30, 35, 40, and 45 dB(Z). The aircraft flight track from 0100-0200 GMT is indicated by the solid line, and the analysis box is denoted by the thick solid line. The origin of the coordinate system is located at the storm center, and the aircraft positions and radar have been plotted relative to the storm center. Coordinates are east-west distance, X, and north-south distance, Y, from the storm center. The tick marks are 24 km apart. The radar position at Galveston is at the center of the cross-hatched circle.

estimates into a time-height grid with a vertical resolution of 300 m and a temporal resolution of 6 s (≃600 m along the flight track). When more than one reflectivity estimate was mapped to a particular grid element, the average reflectivity (Z) was computed and used as the best estimate for that grid element.

Vertical velocity cross sections were constructed by mapping the vertical incidence Doppler radial velocities into a time-height grid identical to that used for the reflectivity cross sections. The vertical air velocity (w) was determined from the measured mean Doppler vertical velocities (W) using a technique similar to that described by Rogers (1964). Rogers reasoned that in the absence of vertical air motions, W is a unique function of reflectivity (Z), equal to the mean terminal fallspeed of the precipitation particles (V_t). The difference between W and V_t is a measure of the vertical air velocity (w),

$$w = W - V_t \qquad (1).$$

V_t (m s^{-1}) can be estimated from Z (mm^6 m^{-3}) as follows:

$$V_t = 2.6\ Z^{.107} \quad \text{for altitudes <5 km,} \qquad (2)$$

$$V_t = 0.817\ Z^{.063} \quad \text{for altitudes >7 km,} \qquad (3)$$

and a linear combination of the two relations at altitudes from 5-7 km. The first relationship is from Joss and Waldvogel (1970) and is for rain. The second formula was derived by Atlas et al. (1973) from the snow measurements of Gunn and Marshall (1958). These relationships are applicable at ground level. To apply them at other altitudes, these equations are multiplied by the density-height correction factor ($\rho_o/\rho(z)$) suggested by Foote and du Toit (1969), where ρ_o = 1.1904 X 10^{-3} g m^{-3}, $\rho(z) = \rho_o \exp[-z/9.58]$, and z is altitude in km. The density-height relationship was taken from Nuñez and Gray's (1977) composite Atlantic hurricane thermodynamic structure within 2 deg radius of the center.

Dual-Doppler analyses of the winds in Alicia have been carried out for the box in the northwest quadrant of the eyewall, outlined in Fig. 1, using the technique described by Marks and Houze (1984) and modified by Jorgensen and Marks (1984). Wind analysis for the box was constructed from the tail radar data obtained on the northeast-southwest flight leg (0108-0115 GMT) and the northwest-southeast leg (0148-0155 GMT). The grid elements used in this analysis were 1 km X 1 km in the horizontal and 0.7 km in the vertical starting at 0.5 km altitude. This box had ideal viewing angles for the dual-Doppler analysis, since the legs were nearly perpendicular; however, since the time elapsed between the two legs was 33-47 min, only the steady component of the circulation during this period could be resolved.

Vertical velocity was computed kinematically by upward integration of the anelastic continuity equation [Equation 4 in Jorgensen and Marks (1984)] with kinematic boundary conditions of w=0 at the earth's surface, and at the height where the reflectivity goes to zero. This procedure is equivalent to the special case of the two radar variational integral constrant described by Ray et al. (1980), where the divergence adjustment is constant with height, and the w adjustment is linear with height.

Within the analysis box, 3-dimensional time-composite reflectivity patterns were constructed from the tail radar reflectivity data in the manner described by Marks and Houze (1984) and Jorgensen and Marks (1984). The grid elements used were identical to those used in the wind analysis.

4. VERTICAL CROSS SECTIONS

Figures 2 and 3 show the time-height cross sections of reflectivity and vertical velocity across the eyewall along the two radial flight legs used in the construction of the 3-dimensional wind and reflectivity analysis. The cross sections clearly delineate the two types of precipitation formation regimes discussed by Marks (1984) in the study of Hurricane Allen: (1) a convective regime in the eyewall, and (2) a non-convective or stratiform regime outside the eyewall (farther away from the storm center).

The eyewall reflectivity and vertical velocity patterns were aligned vertically, with updrafts of 5-8 m s^{-1} along the inside edge (closest to the center) and downdrafts of 3-5 m s^{-1} radially outward from the updraft, near the position of the reflectivity maximum. The position of the up- and downdrafts with respect to the reflectivity maximum was consistent with that described by Jorgensen (1984) from aircraft flight level data.

As noted by Jorgensen (1984) and Marks (1984), the strongest reflectivity in the eyewall was below 5-6 km altitude, and the reflectivity maximum sloped radially outward with height. The updraft maximum also sloped radially outward with height until at an altitude of 6-7 km it was directly above the low-level reflectivity maximum. The updraft maximum was composed of discrete cores (or bubbles) of positive vertical velocity, with the strongest upward motion (>10 m s^{-1}) at high altitudes (>8 km) in the ice. Downdrafts were correlated with local reflectivity maxima, and the strong downdrafts (<-3 m s^{-1}) were confined below 6 km.

The non-convective region, radially outward from the eyewall, had a more horizontally homogeneous or stratified reflectivity and vertical velocity structure. The reflectivity pattern was characterized by a "bright band" at 4.8 km altitude, with a sharp drop-off in reflectivity above that altitude. The magnitude of the reflectivity was 20-26 dB(Z).

The vertical velocities in the non-convective region were weaker than those in the eyewall. The vertical velocity pattern was stratified with generally weak downward motion (peaks of 2-3 m s^{-1}) below the bright band (~5 km altitude), and weak ascent (peaks of 2-3 m s^{-1}) above the bright band. As in the eyewall, the peak downdrafts were correlated with the local reflectivity maxima.

Average vertical velocities were calculated from each cross-section for the areas above and below the bright band (delineated in Figs. 2a and 3a) to determine the magnitude of the mesoscale up and down motions, respectively. In the cross-section shown in Fig. 2, the average mesoscale downdraft was 0.3 m s^{-1} and the average mesoscale updraft was 0.36 m s^{-1}. In the cross-section shown in Fig. 3, the average mesoscale up- and downdraft were a little stronger than those in Fig. 2; -0.86 m s^{-1} below the bright band, and 1.36 m s^{-1} above. These values of mesoscale ascent and descent are consistent with those deduced in other stratiform rain systems (e.g. Leary and Houze, 1979).

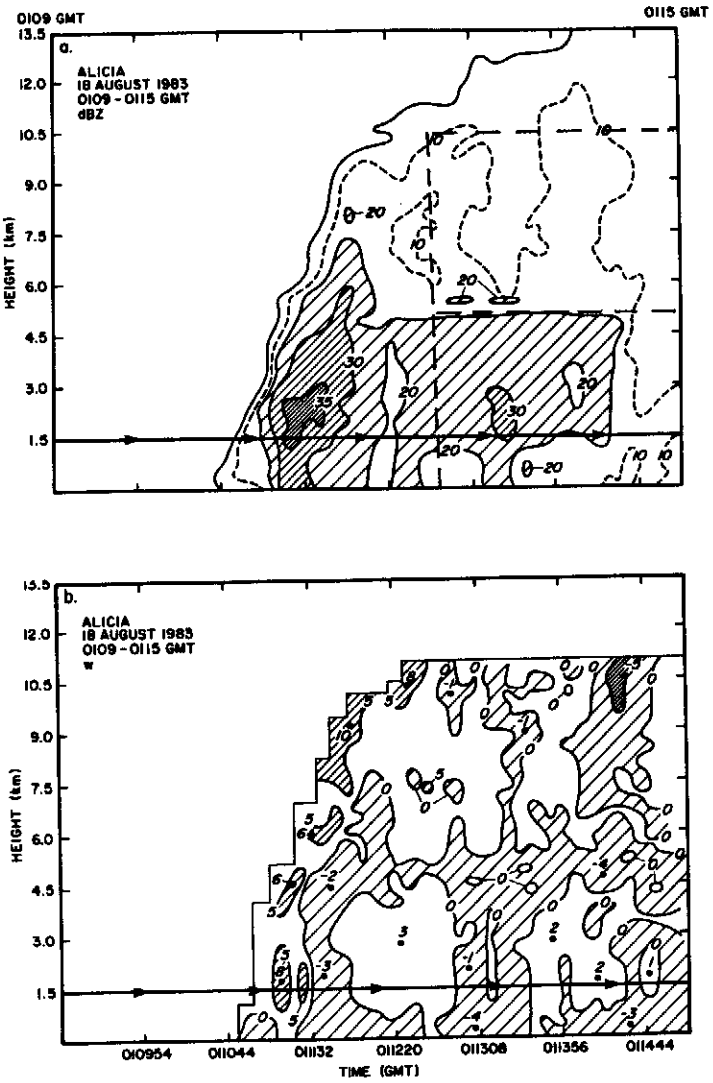

Fig. 2. Time-height cross-sections of (a) reflectivity (dB(Z)) and (b) vertical velocity (m s^{-1}) from the tail radar for 0109-0115 GMT, 18 August. The reflectivity contours are at the minimum detectable signal, 10, 20, 30, and 35 dB(Z). The vertical velocity contours are at -5, 0, 5, and 10 m s^{-1}. The tick marks along X are ≈5.5 km apart. The regions used to compute mean vertical velocities above and below the bright band are delineated by dashed lines in (a).

5. RADIAL STRUCTURE OF THE EYEWALL

Mean radius-height sections were constructed from the 3-dimensional wind and reflectivity analysis within the analysis box (Fig. 4). To obtain these sections, the winds at each grid point and altitude were partitioned into tangential (V_θ) and radial (V_r) components, and mapped into 2 km resolution radial bins. The same was done with the reflectivity (Z) and vertical velocity (w). The data in each radial bin were averaged.

In the reflectivity cross section (Fig. 4a), the outward sloping eyewall with the maximum echo intensity at low levels is again evident (cf. Figs. 2a and 3a). The tangential wind maximum (Fig. 4b) exhibits a similar slope and maximum at low-levels. This structure is similar to that obtained from the non-hydrostatic axisymmetric numerical model of Willoughby et al. (1984a) and in composites of flight track wind data (Jorgensen, 1984a, b). The sloping eyewall in the precipitation water content (represented by reflectivity in our analysis) and tangential wind component fields were evident in the model simulations including ice-phase microphysics. These simulations [illustrated by Fig. 8 of Willoughby et al. (1984a)] are assumed to be the most realisticof the model cases. The results of both Willoughby et al. (1984a) and Jorgensen (1984a, b) indicate the maximum V_θ to be offset radially inward from the reflectivity maximum. Our results, however, show the maximum V_θ located radially outward from the reflectivity maximum.

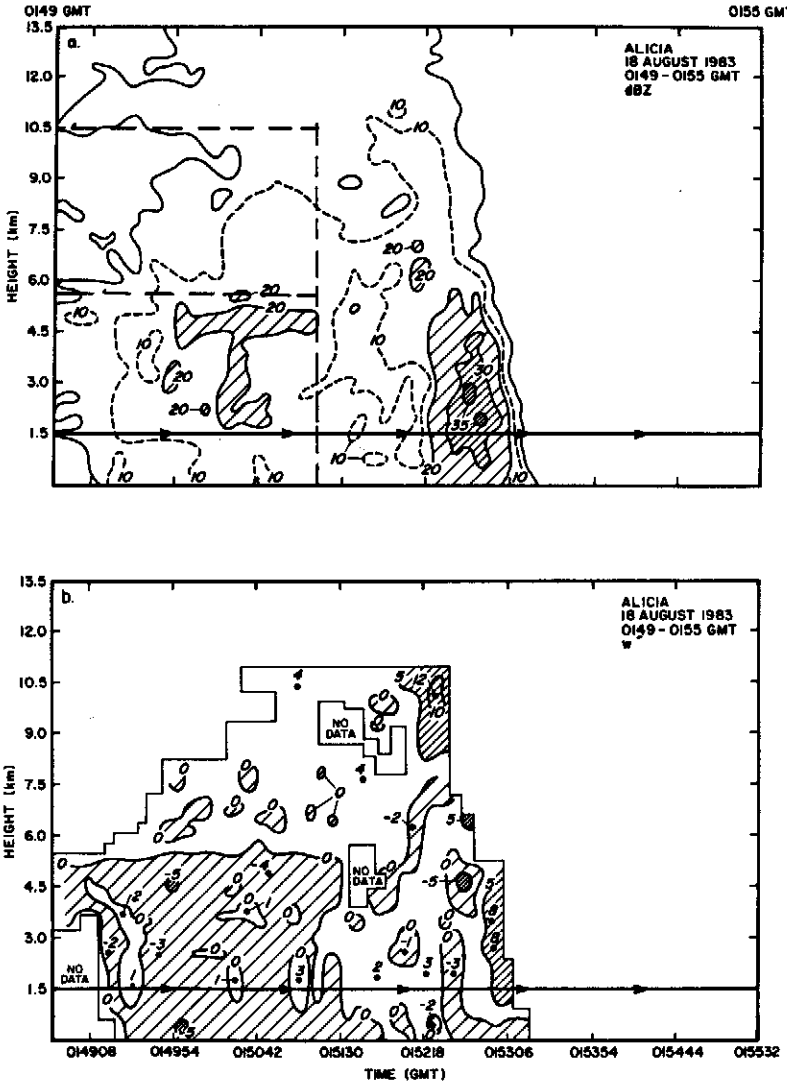

Fig. 3. Same as Fig. 2, except for 0149-0155 GMT, 18 August.

The radial wind component (V_r) field (Fig. 4c) is also generally consistent with the model results of Willoughby et al. (1984a). Most prominent are the radial inflow maxima into the eyewall region at low levels (2-4.5 km) and the shallow layer of intense radial outflow (8-9 m s^{-1}) from the eyewall at 12-14 km height. These features appear both in the model and in our analysis. Our V_r analysis differs, however, from the model results in that the low-level inflow layer does not extend radially outward from the eyewall; beyond 18 km range from the storm center, radial outflow is indicated. However, the model is axisymmetric, while the storm was not symmetric (cf. Fig. 1). Our data were taken on the west side of the hurricane, which has been found by Willoughby et al. (1984b) to be characterized by radial outflow at low levels (1500 m). These interpretations are made with caution since the analysis of the radial wind component is very sensitive to the location of the storm center, which is estimated from flight-level winds (Sec. 3). Since the total horizontal wind is primarily tangential, slight errors in positioning the storm center can lead to significant errors in V_r. We feel that the strong maxima of low-level inflow and upper-level outflow seen in Fig. 4c are qualitatively correct, while the other features remain tentative.

The vertical velocity field in Fig. 4d was computed by averaging the kinematically derived w-values from the dual-Doppler analysis. Because of the simple adjustment technique used to correct the divergence and w at the upper boundary, the magnitude of the vertical velocities in the upper portions of the analysis domain (>9 km altitude) are not reliable. In future reports on this work, these problems will be corrected. For now, we restrict our comments to the analysis below 9 km. At these levels, the mean w field in Fig. 4d confirms the patterns indicated by the vertical incidence observations (Figs. 2b and 3b). The convective updraft motion lies along the inside edge of the eyewall, just above the core of maximum reflectivity (cf. Fig. 4a). Peak velocities are 2-6 m s^{-1}. The downdraft between 10 and 17 km range from the storm center, between the surface and 7 km height, coincides with the region of maximum reflectivity (precipitation). The peak updraft (at lower levels) occurs adjacent to this downdraft.

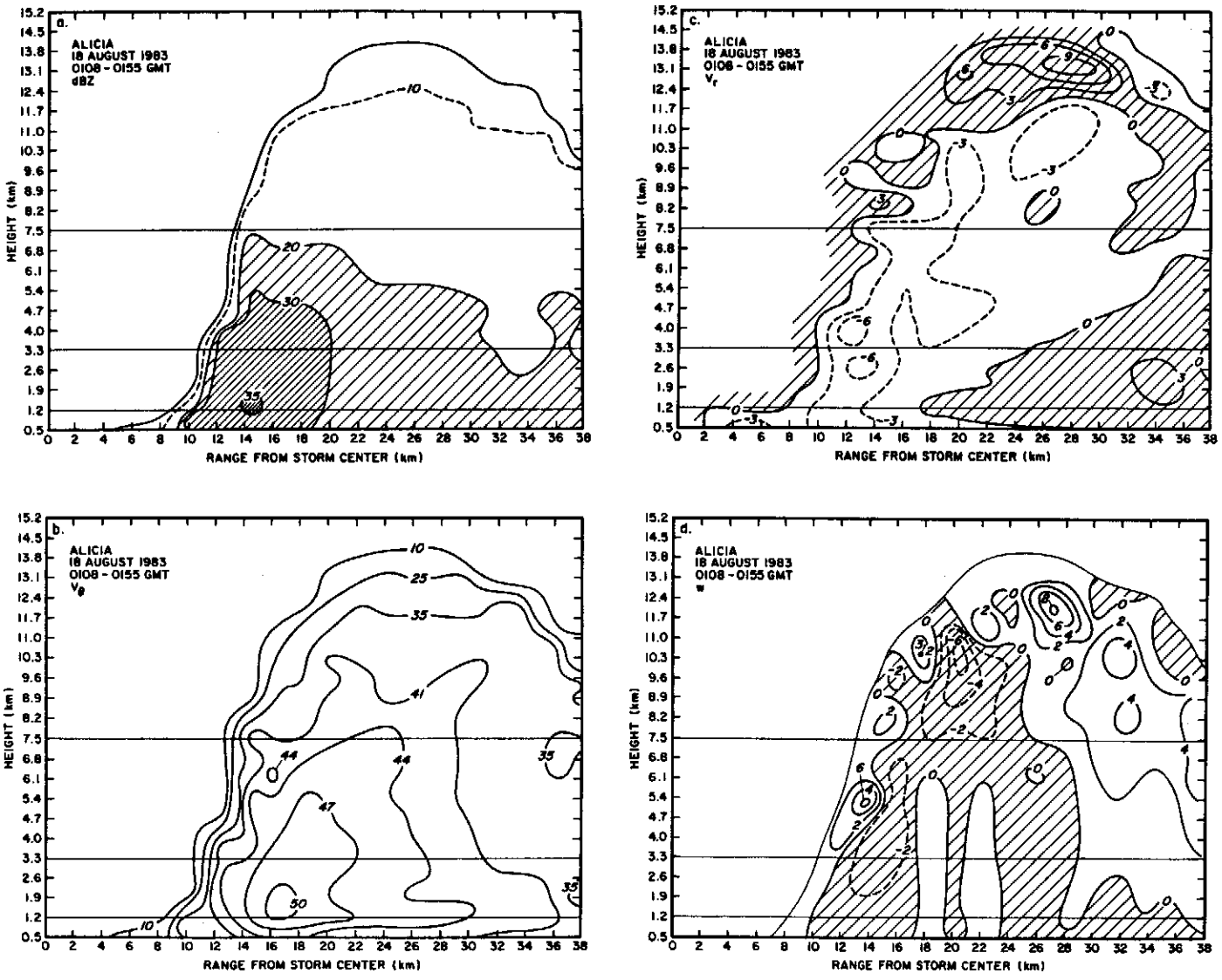

Fig. 4. Radius-height analyses of the azimuthally averaged (a) reflectivity (dBZ), (b) tangential wind speed (m s^{-1}), (c) radial wind speed (m s^{-1}), and (d) kinematically derived vertical velocity (m s^{-1}). Solid contours are positive and dashed contours negative. Positive values (outflow) in (c) and negative values (downdrafts) in (d) are shaded.

6. CONCLUSIONS

Between 0100 and 0200 GMT on 18 August, the NOAA WP-3D aircraft equipped with pulse-Doppler radar flew radial passes across the eye wall of Hurricane Alicia making Doppler measurements in and around the eye wall. Synthesis of the wind field in the eye wall region was derived from the airborne Doppler data.

As in other recently studied hurricanes, the peak echo intensity in the eyewall was below 5-6 km altitude and sloped radially outward with height. Outside the eyewall was a region of stratiform echo exhibiting a bright band. Vertical incidence and dual-Doppler radar analyses showed updrafts in the eyewall also sloping radially outward with height. The core of maximum updraft lay above the reflectivity maximum and appeared to consist of discrete bubbles rising at 5-10 m s^{-1}. A major downdraft coincided with the lower tropospheric reflectivity maximum defining the eyewall, and, in general, downdraft motion was correlated with reflectivity maxima. Mesoscale updraft motion (0.5 - 1.0 m s^{-1} on average) occurred above the bright band in the non-convective region adjacent to the eyewall, while mesoscale downdraft motion of similar intensity was found below the bright band.

The mean tangential wind component maximum in the eyewall region exhibited a structure similar to that of the maximum of radar reflectivity. The maximum values of V_θ were at low levels, and the core of strongest winds sloped radially outward with increasing height.

The mean radial wind component showed strong flow into the eye at low levels and a very shallow layer of strong outflow in the high troposphere.

The reflectivity and wind structure shown by the airborne Doppler radar data in Alicia are generally consistent with the model results of Willoughby et al. (1984a). Thus, confidence is gained both in the physical interpretations provided by their model and in the Doppler radar analysis techniques we have used.

In contrast to our previous study of the developing stages of Hurricane Debby, this study has provided our first opportunity to determine the 3-dimensional wind field of a mature hurricane from airborne Doppler radar data. The results we have obtained (from flight tracks not designed for optimal Doppler observation) indicate the feasibility of this type of research. In future work, we hope to sample the inner core of a mature storm more intensively, while simultaneously obtaining cloud microphysical data with a second aircraft. In this way, we expect to achieve a greater understanding of the precipitation mechanisms, dynamics, and water budget of a mature hurricane.

7. ACKNOWLEDGEMENTS

The data used in this study were gathered with the aid of the NOAA Office of Aircraft Operations flight crews and engineers. Their skill and dedication is greatly appreciated. Dave Jorgensen helped design the Doppler analysis software and provided many helpful suggestions during the course of the analysis. We appreciate many helpful discussions with Mark Powell, Peter Black, Paul Willis, Steve Lord, and Hugh Willoughby. This research was partially supported by the National Science Foundation under Grant No. ATM 80-17327.

8. REFERENCES

Atlas, D., R.C. Srivastava, and R.S. Sekhon, 1973: Doppler radar characteristics of precipitation at vertical incidence. Rev. Geophys. Space Phys., **11**, 1-35.

Case, R.A., and H.P. Gerrish, 1984: Atlantic hurricane season of 1983. Mon. Wea. Rev., **112**, May issue.

Foote, G.B., and P.S. du Toit, 1969: Terminal velocity of raindrops aloft. J. Appl. Meteor., **8**, 249-253.

Gunn, K.L.S., and J.S. Marshall, 1958: The distribution with size of aggregate snowflakes. J. Meteor., **15**, 452-461.

Jorgensen, D.P., 1984a: Mesoscale and convective-scale characteristics of mature hurricanes. Part I: General observations by research aircraft. J. Atmos. Sci., **40**, April issue.

Jorgensen, D.P., 1984b: Mesoscale and convective-scale characteristics of mature hurricanes. Part II: Inner core structure of Hurricane Allen (1980). J. Atmos. Sci., **41**, April issue.

Jorgensen, D.P., and F.D. Marks, Jr., 1984: Airborne Doppler study of the structure and three-dimensional airflow within a hurricane rainband. Preprints 22nd Conference on Radar Meteorology, Zurich, Switzerland.

Joss, J., and A. Waldvogel, 1970: Raindrop size distribution and Doppler velocities. Preprint 14th Conference on Radar Meteorology, Tucson, Arizona, 153-156.

Leary, C.A., and R.A. Houze, Jr., 1979: The structure and evolution of convection in a tropical cloud cluster. J. Atmos. Sci., **36**,437-457.

Marks, F.D., Jr., 1984: Evolution and structure of precipitation in Hurricane Allen. Submitted to Mon. Wea. Rev..

Marks, F.D., Jr., and R.A. Houze, Jr., 1984: Airborne Doppler radar observations in Hurricane Debby. Bull. Amer. Meteor. Soc., **65**, June issue.

Nuñez, E., and W.M. Gray, 1977: A comparison between West-Indies hurricanes and Pacific typhoons. Reprints of the 11th Technical Conference on Hurricane and Tropical Meteorology, Miami Beach, Florida, 528-534.

Ray, P.S., C.L. Ziegler, W. Bumgarner, and R.J. Serafin, 1980: Single- and multiple radar observations of tornadic storms. Mon. Wea. Rev., **108**,1607-1625.

Rogers, R.R., 1964: An extension of the Z-R relation for Doppler radar. Preprints of the 11th Conference on Radar Meteorology, Boulder, Colorado, 158-161.

Willoughby, H.E., and M.B. Chelmow, 1982: Objective determination of hurricane tracks from aircraft observations. Mon. Wea. Rev., **110**, 1298-1305.

Willoughby, H.E., Jin H.-L., S.J. Lord, and J.M. Piotrowicz, 1984a: Hurricane structure and evolution as simulated by an axisymmetric, nonhydrostatic numerical model. J. Atmos. Sci., **41**, March issue.

Willoughby, H.E., F.D. Marks, Jr., and R.J. Feinberg, 1984b: Stationary and propagating convective bands in asymmetric hurricanes. Submitted to J. Atmos. Sci..